phys. stat. sol. (a) **164**, 241 (1997)

Subject classification: 71.35.Cc; 73.40.Gk; 73.61.Ey; S7.12; S7.15

Formation of 10 nm-Scale Edge Quantum Wire Structures and Their Excitonic and Electronic Properties

H. Sakaki, T. Someya, H. Akiyama, Y. Nakamura, N. Kondo, and D. Kishimoto

RCAST/IIS, University of Tokyo, and JST Quantum Transition Project, 4-6-1 Komaba, Meguro-ku, Tokyo 153, Japan

(Received September 23, 1997)

After a brief historical review on edge quantum wire (QWR) structures, we report on our systematic study to prepare and investigate a series of GaAs/AlGaAs and GaAs/AlAs T-shaped edge QWRs. In particular, we examine various features of one-dimensional excitons, such as their binding energy, optical anisotropy, and shrinkage of wavefunctions, and discuss both potentials and challenges of this approach. We describe also our recent work on a novel resonant tunneling structure where electrostatically induced QWR states are involved. We compare this T-shaped QWR approach and its extension to quantum dot structures with other epitaxial growth techniques of nanostructures.

Introduction: Seeds in and Needs for 10 nm-scale Wires and Dots. In 1970, Esaki and Tsu [1] proposed the (layered) superlattice (SL) structure, in which two-dimensional (2D) electrons confined in 5 to 10 nm thick quantum well layers are stacked and coupled to form unique miniband structures. Inspired by this work, one of the authors (H. S.) searched for newer approaches of electron manipulation and proposed in 1975/76 the planar superlattice (P-SL) structure, in which an array of quantum wires (QWRs) or quantum boxes/dots (QBs/QDs) are periodically placed in a planar or linear geometry to control both quantum states and transport properties of one- or zero-dimensional (1D or 0D) electrons [2].

It was noted [2] that these QWR or QD arrays, although difficult or almost impossible to fabricate at that time, would provide a variety of possibilities that cannot be realized in layered SL structures; for example, a) this system enables one to generate a series of peaked density-of-states (DOS) $N(E)$ with true minigap regions ($N(E) = 0$), which lead to enhanced nonlinearities in transport of electrons. In addition, b) this system is compatible with FET (field-effect-transistor) geometries so that both the electron concentration and in-plane potentials can be electrically controllable.

Following this work, a series of proposals and analyses were made to use QWR and QB/QD structures for the manipulation of electrons and holes to realize a variety of unique and desirable properties or functions. They include c) the use of squeezed k-space in single-mode quantum wires to reduce scattering events for the enhancement of electron mobilities [3] and saturation velocities [4], d) the use of peaked DOSs of QWR and QB/QD systems for superior performances of injection lasers [5], e) again, the use of peaked DOSs of these systems for superior performances of quantum-confined Stark

optical modulators [6] and also of carrier induced (or injection) optical modulators [7]. It was also noted that the carrier confinement in QWR and QB/QD structures generally enhances the Coulomb interaction of an electron and a hole and may increase the binding energy E_b of an exciton, when their sizes are reduced to less than the Bohr radius of excitons [8 to 12].

Epitaxial Approaches for 10 nm QWR and QB/QD Structures. The works mentioned above have clearly shown that 10 nm-scale quantum wires and boxes/dots are very attractive both for physics study of 1D and 0D electrons and also for advanced electronics applications. This statement is true, however, only when the technology to fabricate such small wires and dots is developed and made available. Stimulated by these needs, intensive works have been made for the last ten years not only to extend the limit of electron beam lithography and other lithography-based techniques, but also to explore and develop new epitaxial methods, by which 10 nm-scale wires and dots can be grown. Indeed, several promising techniques have been established. Among them, the idea of edge quantum wire (E-QWR), proposed by Sakaki in 1980 [3], is the earliest of such trials; here, the edge surface of a pre-grown QW structure is first exposed and then a barrier structure with positive charges is formed onto it to induce and confine 1D electrons along the edge plane by elecrostatic fields (see Fig. 1a) for a specific example of this type of field-induced E-QWRs. Note that the lateral size of the wire is precisely determined by the thickness d_1 of pre-grown QW layers (QW-1) and can be as accurate as the QW thickness itself. Chang et al. [13] proposed in 1985 a modified version of E-QWR, in which the second QW (QW-2) layer with thickness d_2 is overgrown onto the exposed edge plane of QW-1, as shown in Fig. 1b. Here not only electrons but holes can be confined in the T-shaped intersection of QW-1 and QW-2.

Though these two basic structures of edge QWRs were proposed quite some time ago, their fabrication has become possible only recently as the technique to prepare a clean and flat edge surface of pre-grown QW structure was long difficult. Luckily, Fukui and Ando [14] and Pfeiffer et al. [15] have, respectively, shown that high-quality edge surface of QW structures can be prepared by facet growth [14] and in-situ cleavage [15] of QW structures. By using these techniques, various edge wire structures have been formed and unique properties of quasi-1D systems have been investigated [16 to 22].

In the following, we report on our recent work on a series of T-shaped edge QWRs which have been formed and systematically characterized to disclose

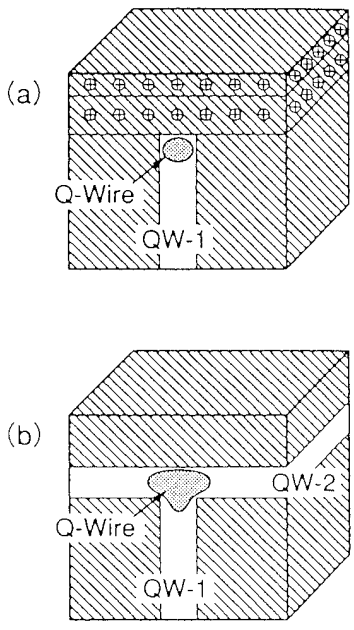

Fig. 1. Two types of edge quantum wires formed on the edge plane of quantum well structures with well width d_1. An example of electric-field induced E-QWRs (part a) confines only electrons or holes, whereas a T-shaped E-QWR (part b) with the overgrown QW2 or width d_2 confines both electrons and holes

the binding energy and other aspects of 1D excitons and electrons [18 to 23]. We then examine E-QWR structures in comparison with other epitaxially grown QWR structures to clarify both advantages and also problems of this E-QWR system; for example, we discuss influences of interface roughness, and possible ways to make E-QWR more compatible with device structures and so on.

1D Excitons in T-Shaped Edge Quantum Wires.

Sample structures and spatially resolved PL spectra. As stated earlier, one attractive aspect of T-shaped QWRs is that their cross-sectional shape can be controlled accurately by the precise setting of the thickness d_1 of pre-grown QW layers (QW1) and that d_2 of an overgrown QW layer (QW2). Using this feature, a variety of GaAs T-shaped QWRs were grown by the cleaved-edge overgrowth technique, originally developed by Pfeiffer et al. [15]. In case of GaAs/AlGaAs T-shaped QWRs, a GaAs layer (QW2) and an AlGaAs barrier layer (with $x = 0.3$) were deposited onto the cleaved (011) plane of a pre-grown epitaxial wafer, which contains not only GaAs/AlGaAs multi QWs but also a thick (2 to 5 μm) AlGaAs layer, as illustrated in the inset of Fig. 2, left part [20].

By sending Ar laser light through an objective-lens optics, we excited a specific position of the sample at 4.2 K and collected photoluminescence (PL) from the same spot with the typcial spatial resolution of 1 to 2 μm and its spectrum was analysed by a standard monochromator. As shown in Fig. 2 left part, when the laser was focused onto the QWR region (region (a) of the inset), the PL showed the spectrum of curve a, which contains two strong peaks and one weak one inbetween. When the laser spot was in the region (b) of the inset, a strong PL weak was observed at 1.59 eV, while two side peaks are quite weak, as shown by curve b of Fig. 2, left part which indicates that the middle

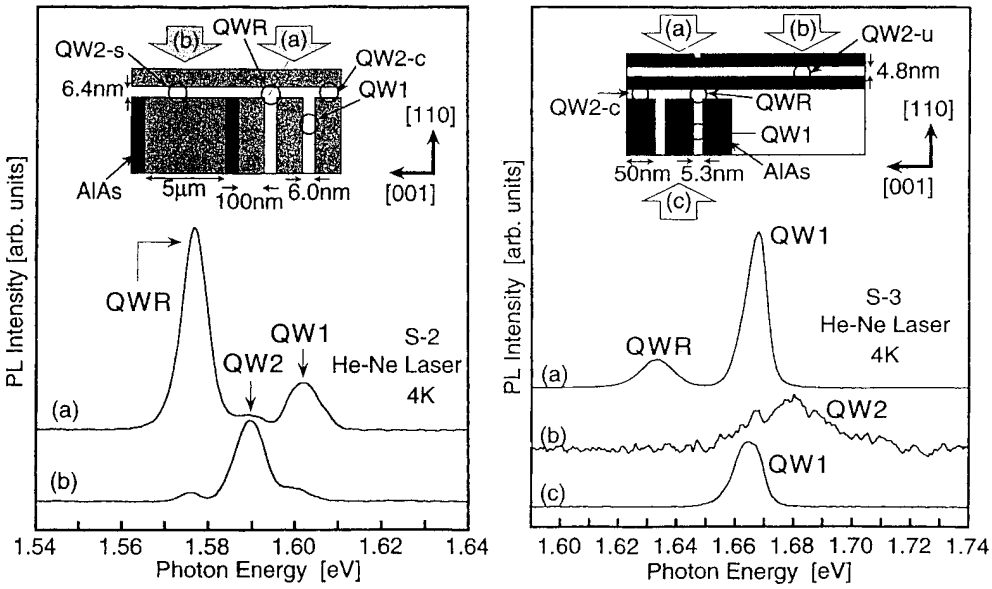

Fig. 2. Photoluminescence spectra from GaAs/AlGaAs T-shaped edge quantum wires (left part) and those from GaAs/AlAs T-shaped edge QWRs (right part). Insets in both figures show schematically the cross sectional shapes of two types of samples

peak originates from 6.4 nm thick QW2. As the highest PL peak was observed also from the pre-grown wafer with no overgrowth, the peak can be attributed to 6 nm thick QW1. Hence, one can conclude that the lowest peak comes from T-shaped QWRs. The validity of such interpretation will be further examined later in section on the next subsection.

Here a remark should be made on the role of carrier diffusion in this system. When the T-shaped QWR structure is excited by an Ar laser, carriers are mostly generated in AlGaAs barriers and flow into neighboring QWs (QW-1, and QW-2). Some of these carriers and/or excitons in QWs recombine radiatively, giving rise to a characteristic PL line of QW-1 or QW-2, but those in the vicinity of QWRs may diffuse and flow into them, luminescing at the ground state energy of the 1D exciton. In partricular, as the spacing between two T-QWRs in the sample of Fig. 2, left part, is only 100 nm, the majority of excitons created in region (a) of QW2 are expected to be collected by the wire region. This is the reason why the PL line resulting from QW2 is quite weak in curve a of Fig. 2, left part and recovers its intensity only in region (b), where the flow of carriers into QWRs is negligible.

Energy levels and exciton binding energy in T-QWRs. It is now clear that in T-shaped edge QWRs, one can separately detect three PL lines, E_{1D}, $E_{2D}(1)$, $E_{2D}(2)$, coming from the QWR, QW1 and QW2, respectively. This set of data allow one to determine precisely the well width (thickness) a of QW1 and that b of QW2, as the Al composition in barrier regions is known. The linewidth study on PL spectra also enables one to evaluate the well width fluctuation, as will be discussed later.

To clarify how PL energies and quantum levels depend on the structural parameters of T-QWRs, a series of GaAs/AlGaAs samples with Al content $x = 0.3$ were prepared [19, 21]. For this S-1 series, a number of wafer pieces were produced from the same pregrown QW1 wafer and, after exposing their cleaved edges, QW2 layers of various well widths d_2 were deposited. The thickness d_1 of QW1 is 5.4 nm, while that d_2 of QW2 is varied between 5.2 and 5.6 nm. Here, d_2 means an "average and effective" thickness of the overgrown QW2 layer, as it is not an integer multiple of GaAs lattice spacing. Photoluminescence spectra of these samples were measured at 4.2 K, and the energies of three PL peaks are plotted in Fig. 3 as functions of "thickness" d_2 of QW2. Note that, when the width d_2 is increased, the energy $E_{2D}(1)$ of the PL line from QW1 remains constant ($= 1.613$ eV), indicating the uniformity of well widths d_1 in the pre-grown wafer. In contrast, PL peaks $E_{2D}(2)$ from QW2 show a steep fall, as expected, and PL peaks E_{1D} from a series of T-shaped QWRs move also toward lower energy.

We now discuss the energy separation $E_{2D} - E_{1D}$ between the QWR PL line and the lower of two PL lines from neighboring QWs. We refer to this quantity as the effective confinement energy, since it is the energy required to bring the 1D exciton in the wire to the 2D exciton state in one of the neighboring QWs. It is clear from Fig. 3 that the effective confinement energy is dependent on the width d_2 of QW2 and it gets maximum (about 18 meV), when PL peak energies from QW1 and QW2 are close to each other. Note here that the coincidence of PL peak energies occurs when the well width of QW2 is slightly thinner than that of QW1 because of the different effective mass of holes on (001) and (110) planes.

This confinement energy consists of three components; the first part comes from the difference between the one-particle ground level energy of a 2D electron in the QW and

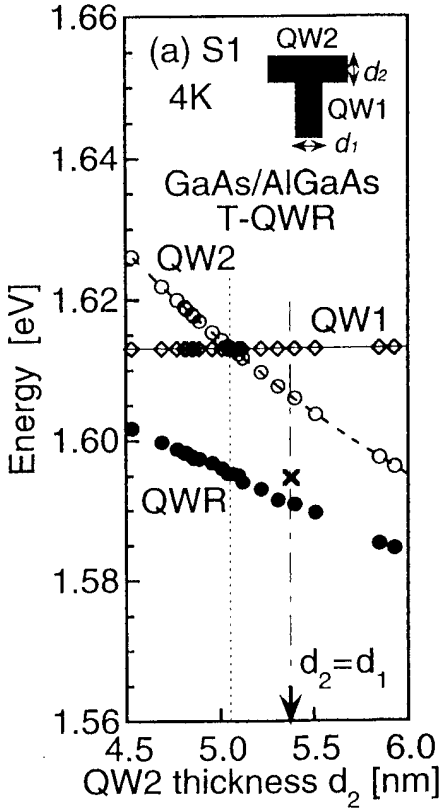

Fig. 3. The energies of the three photoluminescence peaks from QW1, QW2, and T-QWR measured at 4.2 K on a series (S-1) of GaAs/AlGaAs T-QWR structures grown on the cleaved plane of a 5.4 nm thick multi QW wafer are plotted as functions of the well width d_2 of QW2. See the text for details

that of a 1D electron in the QWR. The second component is associated with the spacing of the ground levels of 2D and 1D holes. The third component is the difference between the binding energy $E_b(1D)$ of 1D excitons and $E_b(2D)$ of 2D excitons. By solving the one-particle Schrödinger equation for an electron, one can calculated the first component and find it to be 14 meV for our specific structure. Similarly, the second component associated with 1D and 2D hole states is estimated to be 1 to 2 meV, which is quite small because of the heavy mass of holes. As the measured effective confinement energy $E_{2D} - E_{1D}$ is larger than the sum of the first and the second components by 2 to 3 meV, this difference is ascribed to the third component, that is the enhancement of the binding energy of excitons. If the binding energy $E_b(2D)$ of 2D exciton in a 5.4 nm-thick GaAs/AlGaAs QW is assumed to be about 14 meV, $E_b(1D)$ of 1D excitons in our T-shaped GaAs/AlGaAs QWR is concluded to be 16 to 17 meV. Recently, several theoretical calculations of the binding energy of 1D excitons have been reported [9, 11, 12] and found to explain our experiments on AlGaAs/GaAs T-QWRs successfully.

As an attempt to further increase both the effective confinement energy $E_{2D} - E_{1D}$ and the binding energy $E_b(1D)$ of 1D excitons, another series S-2 of T-QWRs were prepared with AlAs barriers on the cleaved edge of a GaAs/AlAs QW1 wafer with $d_1 = 5.3$ nm. In forming this series, we have employed a modified structure, shown in the inset of Fig. 2, right part. Here two GaAs layers of nominally identical thickness d_2 were overgrown onto the cleaved edge so that another quantum well QW2-u with the same well width was formed just above the usual QW2-c. As shown in Fig. 2, right part. This modified structure allows one to evaluate easily photoluminescence (PL) from GaAs/AlAs QW2-u. This PL spectrum is supposed to be identical to that from QW2, and allows us to shed light on QW2-c without incorporating a thick and vulnerable AlAs layer in the neighborhood of QW1 [19, 20].

By studying the PL spectra of S-2 series, the effective confinement energies $E_{2D} - E_{1D}$ of GaAs/AlAs T-QWRs were also determined by assuming the thickness "d_2" of QW2-u to be the same as d_2 of QW2-c. It is found that the confinement energy thus determined

is dependent on "d_2", as in the case of series S-1, and becomes as large as 38 meV when the well width "d_2" of QW2-u is close to the well width d_1 (5.3 nm) of QW1. To follow the same scheme of data analysis, we calculated the one-particle ground level energies of 1D and 2D electrons and holes for this T-QWR structure, we found that the difference of the ground levels of 2D and 1D electrons is about 23 meV and that for holes is around 2 meV. As the sum of the two is smaller than the measured effective confinement energy by about 10 to 13 meV, this remaining component can be tentatively ascribed to the enhancement $E_b(1D) - E_b(2D)$ of the binding energy of 1D excitons. As we set $E_b(2D)$ to be 14 meV, $E_b(1D)$ is estimated to be 24 to 27 meV, which is remarkably large.

Theoretical calculations of the binding energy of 1D excitons in GaAs/AlAs T-QWRs have been performed by several groups [9, 11, 12] and shown to be around 18 meV for our sample structure. The main reason for the discrepancy is not clarified yet. One of the sources of errors is the oversimplification in the calculation of single-particle energy levels. Another possibility is that the effective thickness of QW2-c might have been slightly thicker than that of QW2-u, for example, by a half or one monolayer. Such an error corresponds to only 3 to 5% of the well width and can be caused either by the roughness of heterointerfaces or by the insufficient controllability of film thickness. Indeed the linewidth of PL peaks is about 15 meV for this sample, suggesting their possible influences. These factors may lead to the overestimation of the exciton binding energy by 6 to 12 meV, which could remove the existing discrepancy. Our work is under way to examine this possibility more in detail.

Optical anisotropy and other features. It is known that the dipole transition between the conduction electron state and heavy hole states in the valence band of usual (001) QWs are optically active for an electric field parallel within the QW or (x, y) plane but inactive for a perpendicular field (parallel to the z-axis). Similarly, the transition associated with heavy hole states confined in a (110) QW on the cleavage plane is optically active for a field along the z-axis as well as for the field along the x- or [1−10] axis, which is parallel to the length axis of T-QWRs.

The character of holes in 1D excitons of our T-QWRs should be reflected in their polarization dependent optical properties [21]. We measured, therefore, at 4.2 K photoluminescence intensities of T-QWRs both for polarization normal to the wire and parallel to it. In Fig. 4, we plot the (anisotropy) ratio of PL intensities measured for two polarization as a function of the thickness d_2 (referred to as b in the figure) of QW2. For comparison, we plot also the anisotropy ratio for QW1 and QW2. It is clear that the ratio is about 0.7 at $d_2 = 8$ nm, but decreases systematically to 0.2, as d_2 is reduced. This indicates that the character of hole states in T-QWR is close to that of QW2 when d_2 is large, but transforms to that of QW1, as d_2 is reduced. Here one should note that the anisotropy ratio measured in QW2 is slightly less than unity; this is reasonable, since the theory predicts it to be 0.8 as a result of the anisotropy in the valence band structure.

Another point of interest in T-QWRs is the spatial extent of the excitonic wavefunction. As discussed earlier, the quantum confinement by a given T-geometry works much more effectively for electrons than for holes because of the differerence in effective masses. Hence, the one-particle eigenstate of holes tends to spread over a wider volume than that of electrons. In the excitonic picture, however, a hole is attracted by a con-

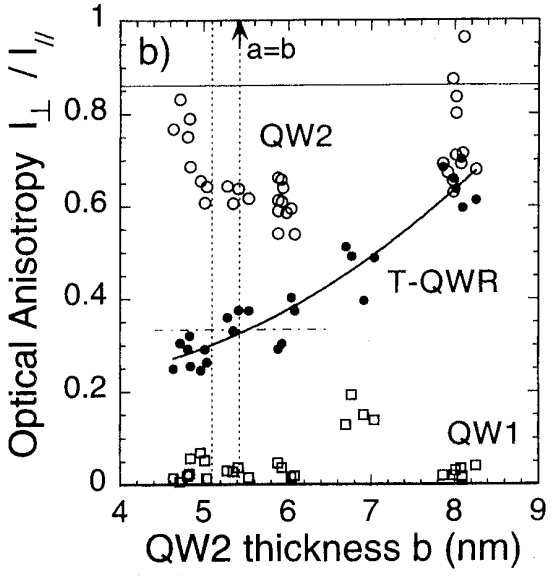

Fig. 4. The photoluminescence (PL) intensities of a series of T-QWRs are measured at 4.2 K for polarization normal to and parallel with the wire and their (anisotropy) ratio is plotted as a function of the thickness d_2 of QW2. For comparison, the anisotropy ratio for PL peaks from QW1 and QW2 are also shown

fined 1D electron and its wavefunction, therefore, will be somewhat squeezed into a smaller volume.

One convenient method to assess the spread of the excitonic wavefunction is to study the shift of PL energy in the presence of magnetic fields. In case of 2D excitons, the shift is given by the square of B times the diamagnetic coefficient, that is proportional to the effective area of the excitonic wavefunction. Indeed, this coefficient is found to decrease systematically, as the well width is reduced. In case of QWRs, where the rotational symmetry is broken, extra components play some role and complicate the interpretation. In our T-QWRs, however, the magnetic-field dependence of the PL shift still serves as a measure of the effective area of 1D excitons [18]. It is found that this coefficient gets as small as $0.013\,\mathrm{meV/T^2}$, which is less than the minimum value achievable in 2D systems [18].

Corresponding to the squeezing of wavefunctions by QWRs, one expects that the oscillator strength of spatially squeezed 1D excitons should be enhanced. This expectation has recently been proven by performing PL excitation (PLE) measurements on a series of T-QWR structures [22]. The PLE intensity of a QWR is found to be comparable to that of a neighboring QW in spite of the far smaller volume occupied by the wire. Although quantitative analysis requires more detailed account of non-radiative recombination and other processes, experimental findings indicate that the oscillator strength of excitons is somewhat enhanced by QWR confinement.

Roughness/Defect and Other Issues. Although the edge quantum wire is one of the most reliable approaches for the formation of 10 nm-scale wires, there are several issues to be solved in the future. For example, the interface roughness or the microscopic thickness variations of QW1 and QW2 may cause significant fluctuations in the ground level energy of 1D electrons and holes in T-QWRs. As in the case of usual QWs, the sum $\mathrm{d}E_\mathrm{e} + \mathrm{d}E_\mathrm{h}$ of such effective level fluctuations would determine the linewidths $\mathrm{d}E_\mathrm{PL}$ of PL spectra. Indeed, as seen in Fig. 2, PL linewidths of GaAs/AlGaAs T-QWRs are not negligible (7 meV) when the well widths d_1 and d_2 are 6 and 6.4 nm, respectively. The PL linewidths measured on two series of GaAs/AlGaAs and GaAs/AlAs T-QWRs have shown that the linewidth increases substantially as the QWR confinement is in-

creased either by reducing the well widths d_1 and d_2 of constituent QWs or by increasing the barrier height. For example, as shown in Fig. 2, right part, the linewidth of PL from GaAs/AlAs QWR with $d_1 = 5.3$ nm, and $d_2 = 4.8$ nm is more than 10 meV.

One way to quantify the interface roughness of QWs and/or QWRs is to divide the measured PL linewidth by the sum of the energy level variations of confined electrons and holes calculated for the size variation of one monolayer, as it gives the effective roughness of the interface. By such a procedure, it has been found that both T-QWRs and QW2 grown on (110) planes at 480 to 500 °C have an effective roughness of about 1 to 2 monolayer, while QW1 grown on a (001) substrate at 580 to 600 °C have an effective roughness of 0.25 monolayer, if grown with interruption, and 1 monolayer, if grown without it. Hence, one can conclude that the PL linewidths of QWRs are predominantly determined by the roughness of GaAs QWs grown on a (110) plane.

The interface roughness results in not only the broadening of PL lines from QWRs but also the localization of 1D excitons along the wire and the suppression of the diffusion flow of 2D excitons from neighboring regions of QWs into the QWR region. Indeed, when the sample temperature is raised from 4.2 to 20 K, the PL intensity of T-QWRs increases substantially while that of neighboring QW1 decreases, indicating the importance of such diffusion process. The localization phenomenon of excitons in this system need to be studied more in detail, as it also plays an important role in the correct interpretations of the binding energy of excitons as well as various optical properties, including the laser action of this system.

The second issue to be addressed is the significant decay of PL from T-QWRs often seen in the temperature region above 100 K. This indicates that QW-2's grown on the (110) plane tend to contain a higher concentration of impurities and/or defects, which work as non-radiative centers. This is quite reasonable, as GaAs and AlGaAs layers grown at lower temperatures are known to incorporate higher concentrations of less volatile impurities. Hence, it is quite important to minimize the incoming flux of impurities during the growth by refining not only the quality of the vacuum but also the purity of molecular beams.

Exploration of New E-QWR Structures and New Functions: Field-Induced Edge QWRs on Facets and Resonant Tunneling. In addition to the reduction of interface roughness and defects discussed in the previous section, there are several important challenges to be made with T-QWR and other edge QWR structures. For example, the energy separations between the ground states of electrons and holes in a T-QWR and those excited states in the QWR or in neighboring QWs cannot be made far greater than 20 to 30 meV, even though such large spacings are desirable in many practical devices. Hence, better T-QWR structures must be designed and realized. T-QWR structures containing strained InGaAs layers as studied first by Gershoni et al. [37] may be an attractive candidate. Another important challenge is to improve the device prospect of edge QWR structures by exploring ways to prepare them with no resort to the cleavage process. A third is to explore new types of edge QWR structures with which new device functions are achieved. Here, we briefly describe a novel edge QWR structure, in which two of such challenges are made.

The structure described here is a novel resonant tunneling structure [23], which is schematically shown in Figs. 5a, b and c. Here, the edge plane of a 20 nm thick n^+-GaAs QW is in face with a thick n^+-GaAs counter electrode via a double-barrier struc-

ture [23], which consists of nominally 7 nm thick AlGaAs barriers and a 6 nm thick undoped GaAs QW. The whole structure could have been prepared with the cleaved edge overgrowth technique, as shown in Fig. 5a. In our recent work, however, we have used the selective MBE growth technique on a patterned GaAs substrate with mesa stripes, which results in a trapezoidal structure having two (111) side planes and a (001) top plane [14, 24, 25]. The facet is formed under a growth mode, where deposited Ga atoms migrate efficiently over the surface and are preferentially incorporated on the top (001) surface. By depositing under this condition a nominally 20 nm-thick Si-doped GaAs layer sandwiched by two AlGaAs barriers, a novel n^+-QW electrode structure has been formed with one edge plane being exposed as shown in Fig. 5b. On top of this structure, we have formed under another growth condition consecutively an AlGaAs/GaAs/AlGaAs double-barrier structure and a 3D n^+-GaAs electrode.

The novel resonant tunneling diode thus prepared is unique in that electrons change dimensions between 3D and 2D as they move from one electrode to the other. An even more interesting aspect is that a quantum wire state is involved in this transport, since

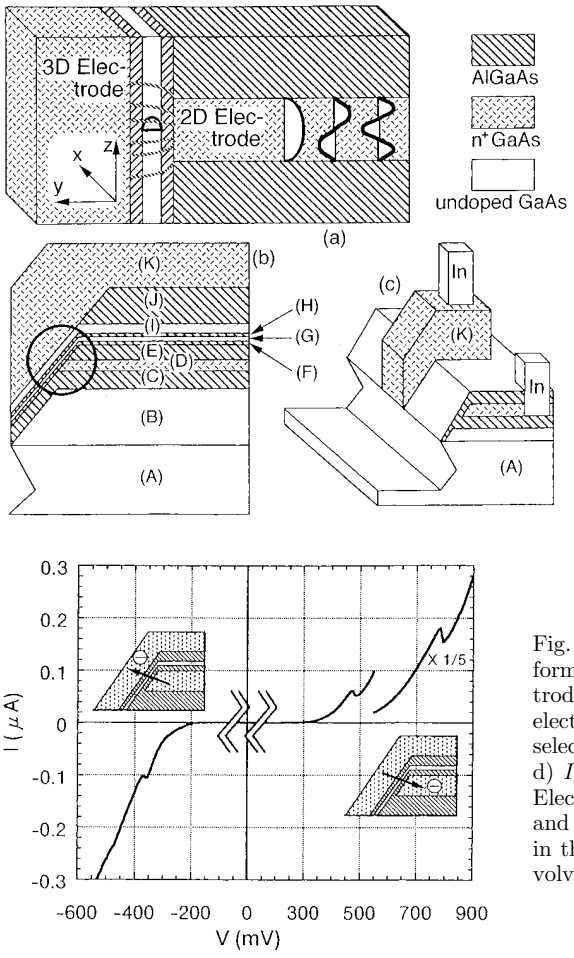

Fig. 5. A novel resonant tunneling diode a) formed on the edge plane of a doped 2D electrode by growing a double barrier and the 3D electrode. The device structure formed by the selective facet growth is shown in b) and c). d) *I–V* characteristics of this device at 4.2 K. Electrons flow between 2D and 3D electrodes and quasi-1D states induced electrostatically in the middle QW by the bias voltage are involved in the transport

the electron wave tunneling from the 3D electrode into the QW is subject to a converging electric field and may well be confined, as shown in Fig. 5a. In fact, the self-consistent solution of the Schrödinger and Poisson equations has shown that 1D QWR states are electrostatically formed and play important roles in the resonant tunneling of electrons.

Current–voltage (I–V) characteristics of our novel RT diode have been measured at 4.2 K. As shown in Fig. 5d, a negative resistance is clearly seen in both polarities. The positions of these NR peaks are consistent with theoretical predictions, suggesting the role of 1D electronic states. In addition, I–V characteristics have been studied in the presence of in-plane magnetics fields and have shown that unique quantum states are indeed involved in this novel diode structure.

Summary and Prospects. Below we briefly discuss key features of E-QWR structures in comparison with other epitaxial methods, such as ridge and groove QWRs and tilted superlattices (TSLs). We discuss also two extended schemes of edge overgrowth technique for the formation of QB structures and their comparison with self-assembled growth of QBs.

Recently, a lot of works have been done to form 10 nm-scale QWRs either in the bottom region of sharp grooves or in the top region of sharp ridges by epitaxy on patterned substrates [24, 26 to 30]. This approach is attractive, since it not only provides 10 nm-scale wires, but it is a semi-planar process (in the sense that QWRs can be buried) and is compatible with many device processing steps, b) it allows the stacking of wires at arbitrary positions. One major issue of this groove/ridge QWR is that their shape or cross section is influenced by the sharpness of grooves and ridges and also by the selectivity of growth rates on crystallographic planes, both of which depend critically on growth conditions. Hence, the controllability of the cross sectional shape of groove/ridge wires is yet inferior to that of T-wires and, hence, needs to be improved.

Tilted superlattices (TSL) formed by the alternate deposition of 0.5 monolayer GaAs and AlAs along quasi-periodic steps on a vicinal substrate are quite attractive in the sense that a large number of (coupled) quantum wires are formed over the entire wafer with no resort to lithography and without spoiling the planarity of the wafer [31 to 34]. However, the quality of GaAs/AlAs TSLs really grown is far lower than that of edge QWRs, since the periodic modulation of compositions is far weaker than the intended level, as it is reduced by random parts of modulation as well as in-plane grading or mixing of compositions. Although TSLs with much higher quality are found to be grown by depositing 0.5 monolayers of InAs and GaAs onto a (110) vicinal plane of a InP substrate [34], continuing effort for the quality improvement is indispensable for the TSL approach to be practical.

Finally, we discuss briefly the role of the edge overgrowth approach for growing high-quality quantum dot or box (QD/QB) structures. Though self-assembled InAs QD/QBs have attracted wide attention recently because of their ease of fabrication and compatibility with other device processings, the dot positions are usually quite random and their size have some distribution [35]. Hence, new methods to grow higher quality QD/QB structures are desired especially to control inter-QD/QB couplings and also to generate a sharply peaked density of states.

It was noted some years ago by one of the authors (H. S.) [36] that the exposure of an edge cross section of a TSL structure, i.e. a coupled QWR array, and the subsequent overgrowth of an n-AlGaAs layer or a GaAs/AlGaAs QW structure onto it leads to a

linear array of QD/QB structures with period corresponding to that of the original TSL structure. It was also noted by the Bell lab group [17] that the exposure of an edge cross section of T-shaped quantum wire structures (instead of a TSL) and the subsequent overgrowth of appropriate structures results in a linear and periodic array of QB/QDs. In fact, the second scheme has been recently tested by Wegscheider et al. [17] and shown to provide a well-defined QD/QB state. This approach will soon open a new field, where the coupling of 10 nm-scale dots is studied and exploited.

References

[1] L. Esaki and R.Tsu, IBM J. Res. Develop. **14**, 61 (1970).
[2] H. Sakaki, K. Wagatsuma, S. Saito, and J. Hamasaki, Thin Solid Films **36**, 497 (1976).
H. Sakaki and T. Sugano, J. Jpn. Soc. Appl. Phys. (Oyo Butsuri) **44**, 1131 (1975).
[3] H. Sakaki, Jpn. J. Appl. Phys. **19**, L735 (1980).
[4] T. Yamada and J. Sone, Phys. Rev. B **40**, 6265 (1989).
[5] Y. Arakawa and H. Sakaki, Appl. Phys. Lett. **40**, 893 (1982).
[6] D. A. B. Miller, D. S. Chemla, S. Schmitt-Rink, Appl. Phys. Lett. **52**, 2154 (1988).
[7] H. Sakaki, K. Kato, and H. Yoshimura, Appl. Phys. Lett. **57**, 26 (1990).
[8] L. V. Keldysh, phys. stat. sol. (a) **164**, No. 1 (1997).
R. J. Elliot and R. Loudon, J. Phys. Chem. Solids **8**, 382 (1959); **15**, 196 (1960).
[9] F. Rossi, G. Goldoni, and E. Molinari, Phys. Rev. Lett. **78**, 3527 (1997).
[10] E. Molinari, phys. stat. sol. (a) **164**, No. 1 (1997).
F. Rossi and E. Molinari, Phys. Rev. Lett. **76**, 3642 (1996), and references therein.
[11] D. Brinkmann and G. Fishmann, phys. stat. sol. (a) **164**, No. 1 (1997).
[12] T. L. Reinecke, private communication.
[13] Y. C. Chang, L. L. Chang, and L. Esaki, Appl. Phys. Lett. **47**, 1324 (1985).
[14] T. Fukui and S. Ando, Electron. Lett. **25**, 410 (1989).
[15] L. Pfeiffer et al., Appl. Phys. Lett. **56**, 1697 (1990).
[16] W. Wegscheider et al., Phys. Rev. Lett. **71**, 4071 (1993).
[17] W. Wegscheider, phys. stat. sol. (a) **164**, No. 1 (1997).
[18] T. Someya, H. Akiyama, and H. Sakaki, Phys. Rev. Lett. **74**, 3664 (1995).
[19] T. Someya, H. Akiyama, and H. Sakaki, Phys. Rev. Lett. **76**, 2965 (1996).
[20] T. Someya, H. Akiyama, and H. Sakaki, J. Appl. Phys. **79**, 2522 (1996); Appl. Phys. Lett. **66**, 3672 (1995).
[21] H. Akiyama, T. Someya, and H. Sakaki, Phys. Rev. B **53**, R4229 (1996); Phys. Rev. B **53**, R10250 (1996).
[22] H. Akiyama, T. Someya, and H. Sakaki, Phys. Rev. B **53**, R16160 (1996).
[23] H. Sakaki, D. Kishimoto, Y. Nakamura, and T. Noda, Appl. Phys. Lett., submitted.
[24] S. Koshiba et al., Appl. Phys. Lett. **64**, 363 (1994).
[25] Y. Nakamura, M. Tsuchiya, S. Koshiba, H. Noge, and H. Sakaki, Appl. Phys. Lett. **64**, 2552 (1994).
[26] E. Kapon, D. M. Hwang, and R. Bhat, Phys. Rev. Lett. **63**, 430 (1989).
[27] R. Rinaldi et al., Phys. Rev. Lett. **73**, 2899 (1994).
[28] Y. Nagamune et al., Phys. Rev. Lett. **69**, 2963 (1992).
Y. Arakawa, Solid State Electronics **37**, 523 (1994).
[29] D. Y. Oberli, F. Vouilloz, and E. Kapon, phys. stat. sol. (a) **164**, No. 1 (1997) and referererences therein.
[30] H. Akiyama et al., Phys. Rev. Lett. **72**, 924 (1994).
[31] P. Petroff, A. C. Gossard, and W. Wiegmann, Appl. Phys. Lett. **45**, 620 (1984).
[32] M. S. Miller et al., Phys. Rev. Lett. **68**, 3464 (1992).
[33] L. Sfaxi et al., Solid State Electronics **40**, 271 (1996); Surf. Sci. **361/362**, 860 (1996), and references therein.
[34] Y. Nakata et al., J. Cryst. Growth **175/176**, 168 (1997).
[35] D. Leonard et al., Appl. Phys. Lett. **63**, 3203 (1993).
[36] H. Sakaki, unpublished (Patent Application, filed (1992)).
[37] D. Gershoni et al., Phys. Rev. Lett. **65**, 1631 (1990).